Magnesium underpotential deposition from nitrate melts and alloy formation with platinum substrate

V. S. Cvetković[1], J. N. Jovićević[1]*, L. J. Bjelica[2]

[1]*Institute of Chemistry, Technology and Metallurgy, Department of Electrochemistry, University of Belgrade, Njegoševa 12, 11000 Belgrade, PAK 125213, Serbia*
[2]*Faculty of Sciences and Mathematics, University of N. Sad, Trg Dositeja Obradovića 3, 21000 N. Sad, Serbia*

Abstract

This paper investigates magnesium underpotential deposition on platinum electrodes from magnesium nitrate-ammonium nitrate melts at temperatures ranging from 400 to 500 K. Electrochemical techniques used were linear sweep voltammetry and potential step. Electrode surfaces were studied by Scanning electron microscopy (SEM), Atomic force microscopy (AFM), Energy dispersive spectrometry (EDS), energy dispersive X-Ray spectroscopy (EDX) and X-Ray diffraction (XRD). In the underpotential range studied, it was found that magnesium underpotential deposition took part simultaneously with reduction processes of nitrate and nitrite. EDS and XRD measurements showed clear evidence of $MgPt_3$, Mg_3Pt alloys being formed.

K e y   w o r d s: magnesium/platinum alloys, underpotential deposition, magnesium nitrate--ammonium nitrate melts, microscopy and microanalysis techniques

1. Introduction

Over the past decade, a great deal of effort has been focused on the ratio of magnesium alloys mass and strength [1, 2]. Magnesium alloys as materials with low density and high strength-to-mass ratio, good fatigue, and impact strength have a wide application prospects in the automotive industry, aerospace, electronic engineering, as well as in electrode components for chemical power sources and rechargeable magnesium battery systems [3–5]. Recently, it has been shown that magnesium alloys, due to their outstanding biocompatibility and biodegradability [6], can be used in the fabrication of biodegradable implants.

Magnesium alloys are presently accounting for only 1 % of the total market for light metal castings. On the other hand, electrodeposition of magnesium and its alloys as a highly efficient production, including innovative processing of Mg-alloys, could become a key factor in cost saving initiatives [7]. However, the electrodeposition of Mg and Mg-based alloys from aqueous solutions is impossible, because hydrogen is generated at the working cathode before magnesium can be deposited. This prevents even the smallest amounts of magnesium metal to remain as a deposit on an electrode without being dissolved in the aqueous solution. In addition, Mg cannot be deposited from solutions of simple Mg salts such as $Mg(ClO_4)_4$ in conventional organic solvents (acetonitrile, propylene carbonate or dimethylformamide). This is most likely due to the working electrode surface becoming covered by passivating surface films whose ionic conductivity is very low [3].

The electrodeposition of Mg is done from melts. Some of these melts include inorganic and organic chloride or fluoride salts, combined with cations of some alkaline/alkaline earth metal, or some organic cation or anion [8–11]. Ionic liquids (made of organic salts) became known relatively recently and proved to be suitable media for electrodeposition of metals and alloys at relatively low temperatures (from 273 to 373 K) [8, 12].

The melts of alkaline and alkaline earth metals nitrate salts, including their possible application as electrolytes [13–15], became a subject of interest in the second half of the twentieth century [16–18]. Among

*Corresponding author: tel.: +381 621796815; fax: +381 113640230; e-mail address: matori47@hotmail.com

some nitrate melts investigated electrochemically, neither magnesium nitrate nor magnesium nitrate – ammonium nitrate mixture melts were studied. The data referencing electrodeposition of magnesium, magnesium underpotential deposition and alloy formation from nitrate melts are practically nonexistent, although their working temperatures should be much lower than in other suitable inorganic melts.

Among reasons for nitrate melts not being investigated very often for metal electrodeposition are very pronounced oxidative characteristics of nitrates and a great number of oxidation/reduction processes that can take place between cations and anions and water which is typically present in nitrates [14, 15], make these melts not conducive for metal electrodeposition. Magnesium nitrate hexahydrate is an octahedral complex with magnesium cation $[Mg(H_2O)_6]^{2+}$ which is very stable. However, it is impossible to remove water from it by heating, because it decomposes before losing water and transforms into magnesium (II) oxide. Finally, the presence of water in magnesium melts cancels the advantages the melts have against magnesium aqueous solutions. Nitrates also pose additional difficulties related to maintaining the intended temperature at ± 3 K, which arise from the large latent heats of the numerous nitrates phase transformations in the temperature range from 373 to 500 K [16].

Metal electrodeposited under underpotential deposition (UPD) conditions (electrodeposition of metals on foreign substrates at potentials more positive than the equilibrium potential of the depositing metal) from aqueous, non-aqueous solutions and melts (even at room temperatures) onto a cathode of a different metal can diffuse into the substrate and generate alloys [19–25]. Alloys obtained by overpotential electrochemical deposition (OPD) and UPD can have different chemical and phase structures from the alloys of the same composition obtained by metallurgical (thermal) methods [8, 20–25]. Recently, magnesium/platinum alloys formation by electrochemical means has been the subject of interest because of their applications in chemical power sources, jewelry and prosthetic aids [3, 4, 5, 6, 26–30].

In this article, we focus on overcoming the limitations of working on electrodeposition from nitrate melts, establishing whether underpotential deposition of magnesium onto platinum from magnesium nitrate exists, and determining whether it leads to magnesium-platinum alloy formation.

2. Experimental procedures

The electrochemical experiments were carried out in a three-electrode electrochemical cell [24, 25] made of Pyrex glass placed in a heating mantle designed for work with melts under a purified argon atmosphere (99.99 % Ar). The temperature of the melts was controlled (via electronic thermostat) between 363 and $463\,\mathrm{K} \pm 3\,\mathrm{K}$. Central neck was closed with a Teflon plug carrying the working electrode (99.999 % Pt plate $0.4\,\mathrm{cm}^2$), left neck with a Teflon plug holding an argon glass inlet-outlet and glass Luggin capillary with magnesium reference electrode (3 mm diameter 99.999 % Mg wire), and right neck with Teflon plug holding magnesium anode (99.999 % Mg) in the shape of a curved rectangular shovel ($7.5\,\mathrm{cm}^2$ active surface area) and a tube of thin glass with a thermocouple. Argon and other possible gases coming out of the cell were captured/washed in two bottles (first with a slightly basic solution and second with a slightly acid solution). The cell setup was placed into a sealed transparent plastic "glove box" to create a moisture free atmosphere around the cell.

The melt used in this work was a non-aqueous eutectic mixture $Mg(NO_3)_2 + NH_4NO_3$. The preparation process of the non-aqueous eutectic mixture $Mg(NO_3)_2 + NH_4NO_3$ has been described in detail elsewhere and briefly stated below [24, 25]. The process of water removal from magnesium nitrate hexahydrate included: 5 g of magnesium nitrate hexahydrate and $15\,\mathrm{cm}^3$ of trimethyl orthoformate brought to a boil and kept for 90 min under reflux at 343 K, followed after 90 min by formation of crystals of non-aqueous magnesium nitrate and remaining liquid being submitted to a vacuum distillation at 343 K. Upon removal of the visible liquid the remaining crystals were vacuum dried for additional 60 min. Non-aqueous magnesium nitrate was kept in a closed glass container in a desiccator furnished with plenty of silica gel. Ammonium nitrate hexahydrate was dried for ten hours at 378 K. Wanted amounts of magnesium nitrate mixture with ammonium nitrate were placed into the cell supplied with electrodes, argon supply was turned on, and the system was heated gradually to the wanted temperature.

Before each measurement, the electrodes, a platinum working electrode, magnesium anode, and a reference electrode were mechanically polished with emery paper (FEPA P-4000) to a mirror finish and then etched. Platinum working electrode (99.999 % Pt) was etched in aqua regia in several intervals of ten seconds alternating with washing with deionized water. Magnesium anode and a reference electrode were etched in the solution, made of conc. HNO_3 + conc. H_2SO_4 + deionized water, in several intervals of ten seconds alternating with washing with deionized water [24]. Finally, all electrodes were rinsed with deionized water, absolute ethyl alcohol, dried and mounted in the cell.

The experiments involved using electrochemical techniques: linear sweep voltammetry (LSV) and potential step. The potentials of working electrodes were measured in relation to the equilibrium potential of
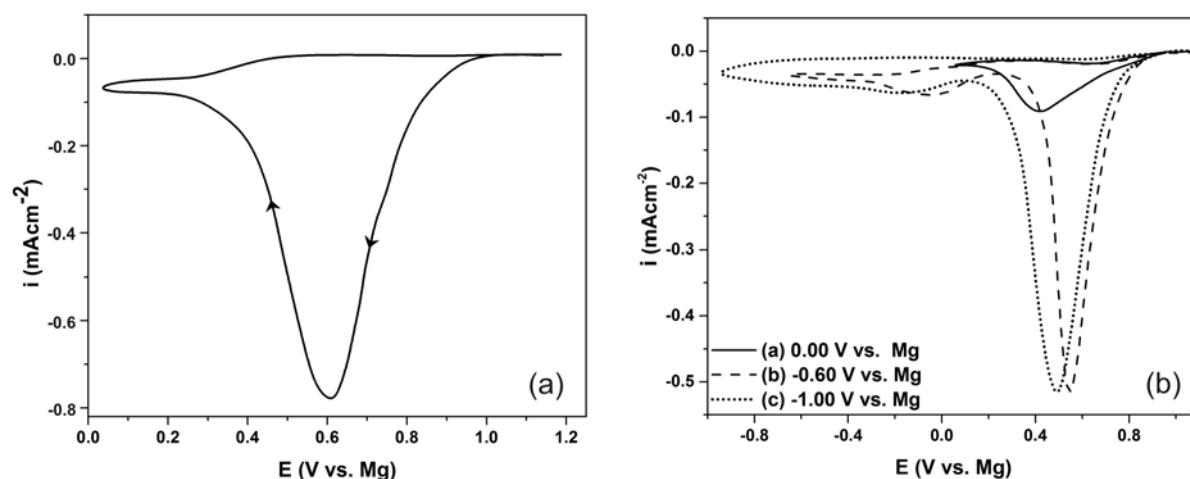
Fig. 1. Cyclic voltammograms recorded on a Pt electrode in non-aqueous eutectic mixture $Mg(NO_3)_2 + NH_4NO_3$ at 450 K, obtained with scan rate $40\,mV\,s^{-1}$; a) $E_s = +1.200\,V \leftrightarrow 0.050\,V$ vs. Mg and b) —) $E_s = +1.100\,V \leftrightarrow 0.000\,V$ vs. Mg; $---$) $E_s = +1.200\,V \leftrightarrow -0.600\,V$ vs. Mg; $\cdots$) $E_s = +1.200\,V \leftrightarrow -1.000\,V$ vs. Mg.

magnesium reference electrode in the melt used under given conditions.

The cyclic voltammetry experiments included one or more cycles of the working electrode potential cycling from a starting potential, E_S (usually 50 to 100 mV more negative than the reversible potential of Pt working electrode) to a final potential, E_F (which was positive to the reversible potential of Mg) and then back again to E_S, all at scan rates (between 5 and 100 mV s^{-1}). Results were recorded by Potentiostat/Galvanostat Princeton Applied Research Corporation Model 273A and controlled by Power Suite Software (Princeton Applied Research).

The potential step method included a change of the working electrode potential from an initial potential, E_I (50 to 100 mV more negative to platinum equilibrium potential in the given melt) to a potential, E_X (50 to 100 mV more positive to magnesium equilibrium potential in the given melt). E_X potential was held constant for 120 and 600 min, after that the cathode was retrieved from the cell under potential to preserve deposited material or possible alloys formed during UPD of magnesium.

After undergoing UPD on platinum, the electrodes were thoroughly washed in the glove box with the absolute ethyl alcohol to remove the melt residue. Then, the sample was transferred out of the box and kept without exposure to the atmosphere. Thus obtained samples were characterized by Scanning electron microscope (SEM) with an Energy dispersive spectroscopy (EDS) (SEM – "JEOL", model JSM-5800, Japan, EDS – "Oxford INCA 3.2", U.K.) and energy dispersive X-Ray spectroscopy (EDX-mapping – Oxford IncaEnergy EDX), X-Ray diffraction using (XRD – "Enraf Nonius powder diffractometer", Germany), Atomic force microscopy (AFM with NanoScope 3D Veeco, USA).

3. Results and discussion

In this work, it was essential to confirm that the method of water removal from magnesium nitrate described above had been effective. It was found that the mass difference between the magnesium nitrate hexahydrate entering the process of water removal and the magnesium nitrate leaving the said process was 39 ± 3 %. This would suggest that at least 92 % of water had been removed. The deviation from 100 % can be attributed to the residual methanol, methyl ester of formic acid or some of their derivatives because the obtained $Mg(NO_3)_2$ crystals appeared to give off these chemicals immediately after drying. In addition, earlier obtained results suggest that the process of water removing from magnesium nitrate hexahydrate was successful [24].

There is no universal reference electrode in experiments with melts. Therefore, in the systems where underpotential deposition is examined it is common practice to use the reversible potential of the depositing metal as a reference electrode potential with an ascribed value of 0.000 V. In the nitrate melts used, for magnesium underpotential deposition on platinum, this meant using magnesium as a reference electrode. Polarization measurements and cyclic voltammetry performed on the magnesium working electrode with magnesium reference, and counter electrodes have shown that reversible magnesium potential in the used magnesium nitrate melts, under temperatures ranging from 340 to 500 K, was stable [25]. The experiments in the non-aqueous eutectic $Mg(NO_3)_2 + NH_4NO_3$ mixture were performed at 450 K and reversible potential of polycrystalline platinum was $1.290\,V \pm 30\,mV$ vs. Mg.

Typical examples of the voltammograms obtained in our system are given in Figs. 1a,b. General charac-

teristics of the voltammograms indicated the presence of more than one reduction peak with no oxidation counterparts. Stripping peaks were not observed even when cathodic end potential was pushed into overpotential range. Sometimes reduction peaks were spread over a wider range of applied potentials without showing a steeper increase or decrease of current density values. Such structures of voltammogram peaks are characteristic of multiple processes which start successively one after the other at potentials whose values are close and proceed further simultaneously (often next process starts with increasing rate at the same time that a previous process ends with a diminishing rate). The obtained peaks then represent the sum of rates of all the processes taking part at a certain potential. The absence of anodic (oxidation) counterparts to the cathodic peaks was a subject of some works [14, 15, 23, 31–33]. These studies emphasize that in nitrate melts changes of the platinum electrode potential from anodic to cathodic values (compared to the magnesium reversible potential) provoke passivation of the working electrode surface which becomes partially (or fully) covered with magnesium oxides layers. These layers do not dissolve when the potential is returned to the starting value.

Suggestions of the possible processes that could produce reduction peaks in the magnesium UPD region investigated, apart from ones brought about by the magnesium underpotential deposition itself, can be found in rare published works [14, 15]. It is important to point out that the potentials of the proposed reactions measured relative to Na, K or Li, cannot be directly used in our case, but it can be assumed with enough certainty that the order of the reaction potentials and the potential differences between these processes were preserved with respect to magnesium reference potential. However, absolute values must be changed by the amounts reflecting differences in reference potentials between Na, K, and Li in their nitrate melts and Mg in used nitrate melts.

Results obtained with linear sweep voltammetry have shown, as it was expected [14, 15, 24], that the first group of anion (nitrate) reduction processes from the non-aqueous nitrate melt used proceed at potentials between ≈ 850 and 350 mV vs. Mg, followed by the second group of nitrate reduction processes at potentials more negative than 350 mV vs. Mg [14, 15, 24] but still in magnesium UPD range. The said reaction potentials are mutually very close, and therefore, the current peaks were smeared over the recorded potential range. The change of the platinum electrode potential from positive values to the magnesium reversible potential (magnesium UPD region), induces some reactions based on nitrogen-based anions and cation, very reactive oxygen anion O^{2-}, OH^- and sometimes water [24] also. All produced gases were removed from the electrochemical cell by the argon
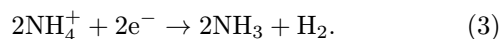
stream, so when the electrode potential is reversed into a positive direction, the theoretically possible reverse oxidation reaction back to initial NO_3^- or H_2O could no longer be expected. As a result, no anodic voltammogram peaks due to the oxidation of the produced gases could be recorded. Furthermore, O^{2-} produced in inner and outer parts of the electrochemical double layer very quickly engaged in reaction with Mg^{2+} present [14, 15, 23, 24, 31–33]:

$$Mg^{2+} + O^{2-} \rightarrow MgO, \qquad (1)$$

the result being the formation of insoluble magnesium oxides in the magnesium UPD region. The thermal decomposition constant [14, 15] decides upon the stability of possibly present magnesium hydroxide:

$$Mg(OH)_2 \leftrightarrow MgO + H_2O. \qquad (2)$$
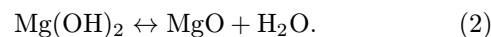
In the melt made of a eutectic mixture of magnesium nitrate and ammonium nitrate, at the temperatures used, ammonium ion, resulting from NH_4NO_3 dissociation [14, 15], forms a compound $(NH_4)_3 Mg(NO_3)_5$. In the melt, this compound exists as a quasi-crystalline structure made of NH_4^+, Mg^{2+} cations, and NO_3^- anions [14, 15]. The fact that the reduction current densities in the magnesium nitrate melts increase with the increase of the ammonium nitrate present, at the constant temperature in the magnesium UP region investigated, leads to the conclusion that NH_4^+ reduction is taking place:

$$2NH_4^+ + 2e^- \rightarrow 2NH_3 + H_2. \qquad (3)$$

However, this reaction is, under conditions given, irreversible and voltammograms could not show oxidation peaks when the electrode potential was reversed in the positive direction.

From the above data, it can be concluded that in the UPD region examined anodic voltammogram peaks cannot be expected.

The half of the work function difference between Pt substrate and depositing Mg is ≈ 450 eV [34] and according to [35] the UPD of magnesium onto platinum should be almost certain. It is logical to assume then that the reduction peaks obtained by LSV measurements on the platinum working electrode from magnesium nitrate and ammonium nitrate melt used in the magnesium underpotential region are sums of partial current densities for Mg^{2+} underpotential reduction, nitrate anion reduction, and ammonium cation reduction. Being a sum, the recorded current densities suggest small magnesium underpotential deposition of partial current densities. Such small current densities exhibited by the UPD voltammograms from similar melts [23, 32, 36, 37] were characteristic of deposited metal mono-
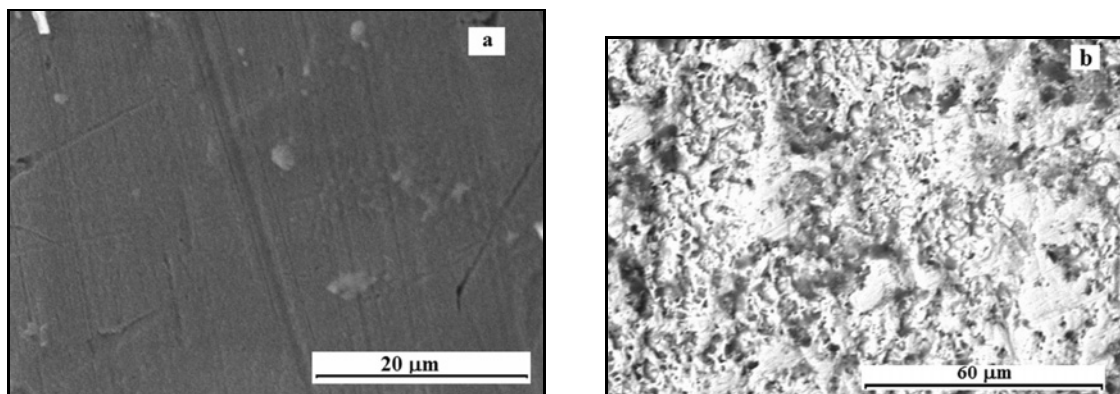
Fig. 2. SEM micrographs of Pt surface after magnesium underpotential deposition at 450 K from non-aqueous eutectic mixture $Mg(NO_3)_2 + NH_4NO_3$ by using potentiostatic technique for a) 2 h and b) 5 h.
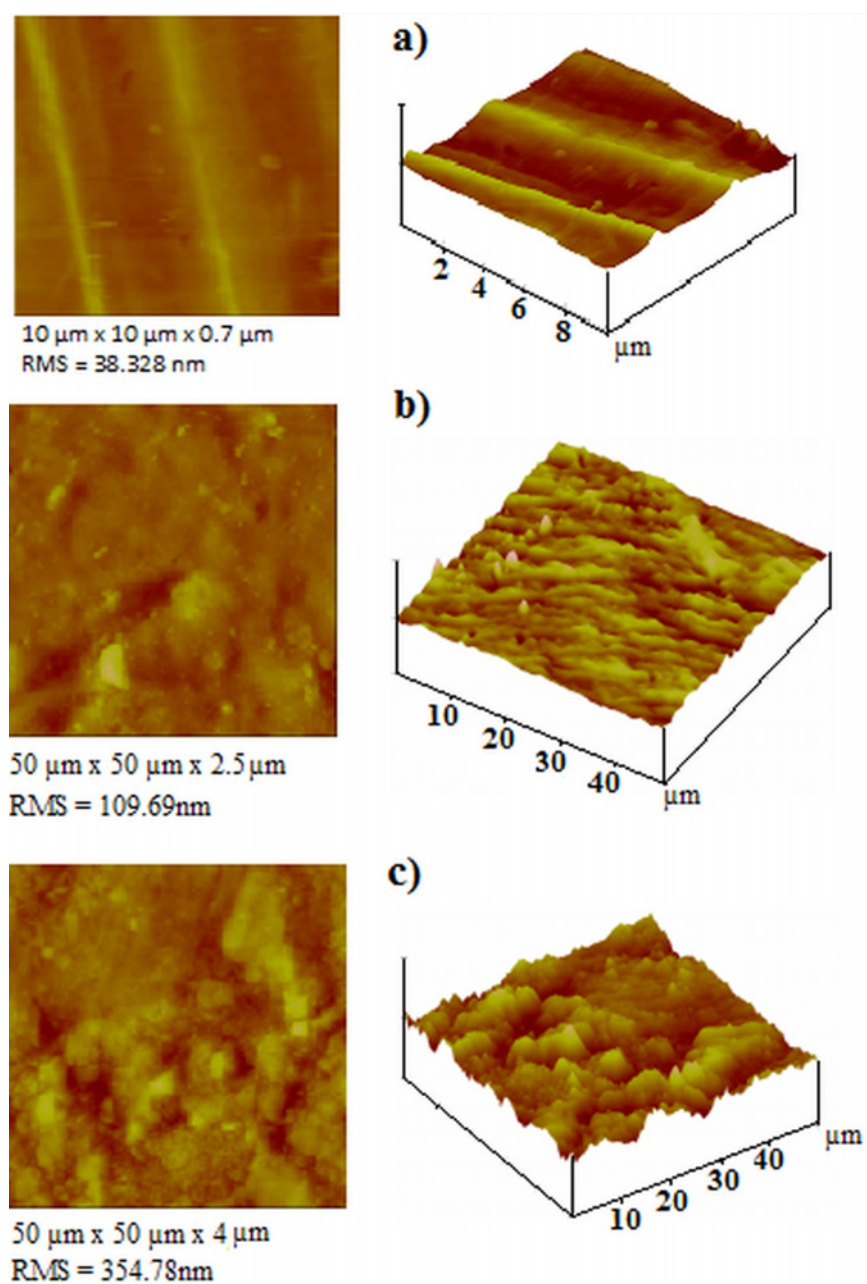

Fig. 3. 2D and 3D AFM images of the platinum surface: a) before magnesium underpotential deposition and after magnesium underpotential deposition at 450 K for b) 2 h and c) 5 h.

T a b l e 1. Results of EDS semi-quantitative analysis for the Pt samples exposed to the constant potential of +60 to +100 mV vs. Mg for 2 and 5 h in used melts

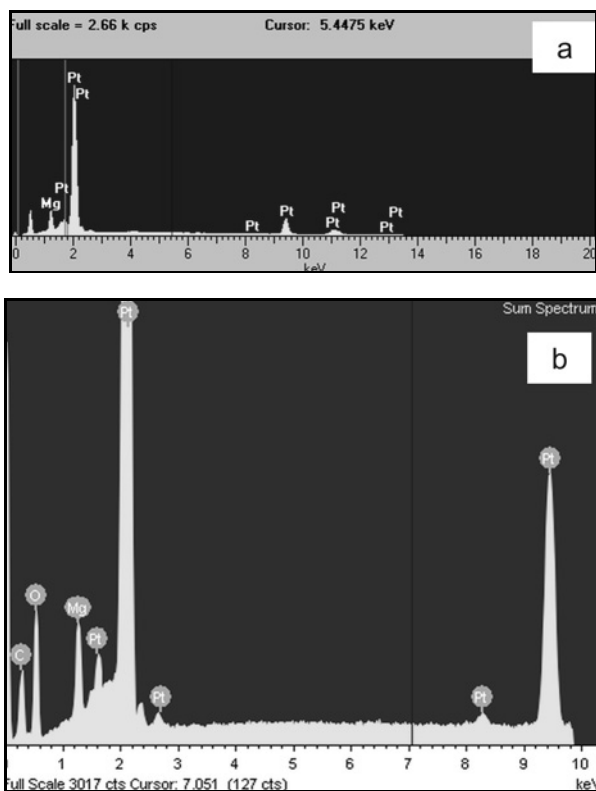|	2 h Mg UPD on Pt substrate			
Elmt.	Spec Type	Elmt (%)	Sgma (%)	(at.%)
O K	ED	30.53	0.14	6.60
Mg K	ED	1.11	0.03	1.56
Pt M	ED	68.36	0.27	1.84
Total		100.0		100.0
	5 h Mg UPD on Pt substrate			
O K	ED	23.40	0.47	3.79
Mg K	ED	3.03	0.04	7.95
Pt M	ED	73.56	0.25	8.26
Total		100.0		100.0

Fig. 4. Characteristic EDS spectra of platinum samples after a) 2 h and b) 5 h of magnesium underpotential deposition at 450 K.

layers diffusing into the substrate and forming alloys.

The indication of magnesium underpotential deposition on platinum is exhibited in Figs. 2–5. They represent SEM, AFM, EDS, and EDX results obtained from the platinum electrode held for two and five hours on electrode potential of +60 mV vs. Mg in the non-aqueous eutectic mixture $Mg(NO_3)_2 + NH_4NO_3$

at $T = 450$ K. A typical example of XRD analysis results for the platinum sample exposed to magnesium underpotential deposition at +80 mV vs. Mg in the same melt and at $T = 450$ K for: a) 2 h and b) 5 h is shown in Figs. 6a,b. In this particular case, the results obtained using XRD analyses suggest that magnesium-platinum alloys are being formed.

The surface of the platinum sample taken after magnesium underpotential deposition at 450 K for two and five hours was analysed by SEM (Fig. 2) and AFM (Fig. 3). The deposits are very compact and significantly rough with agglomerations of different sizes. The roughness and height of the agglomerations increase slightly with increased deposition time.

In Fig. 3a sporadic small areas of rough morphology, probably caused by mechanical interaction during polishing, could be seen on flat and uniform bare platinum surface. The 2D and 3D images in Figs. 3b,c obtained after two and five hours, respectively, of Mg UPD showed crystalline agglomerations, which seem to have a form of islands.

The results obtained by EDS (Figs. 4a,b and Table 1), EDX (Figs. 5a,b) and XRD (Figs. 6a,b and Table 2) analysis of the Pt substrates exposed to constant potentials in the magnesium underpotential region (+50 to +150 mV vs. Mg) strongly suggest that magnesium deposition takes place at potentials more positive than the equilibrium potential of the depositing metal and magnesium-platinum alloys being formed.

It is impossible to identify the precise value of the potential at which magnesium UPD starts. However, it is obviously significantly positive to the reversible magnesium potential in the used melt.

According to the Hume/Rothery rules [38], Mg and Pt fulfill the required conditions to form alloys (solid solutions), including "the 15 % rule", because Mg and Pt atomic radii differ only by 10 %. However, it has been pointed out [26, 44], the phase diagram
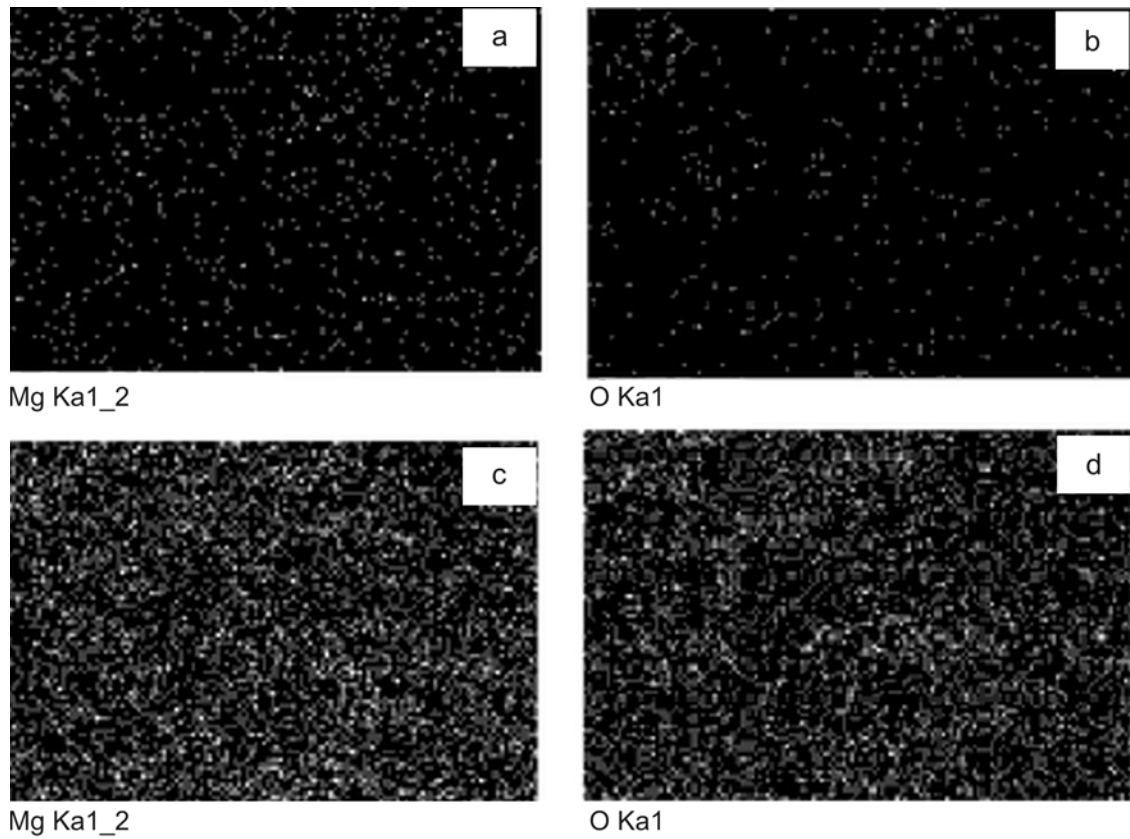
Fig. 5. EDX maps of magnesium a), c) and oxygen b), d) distribution images after two and five hours of magnesium underpotential deposition at 450 K.
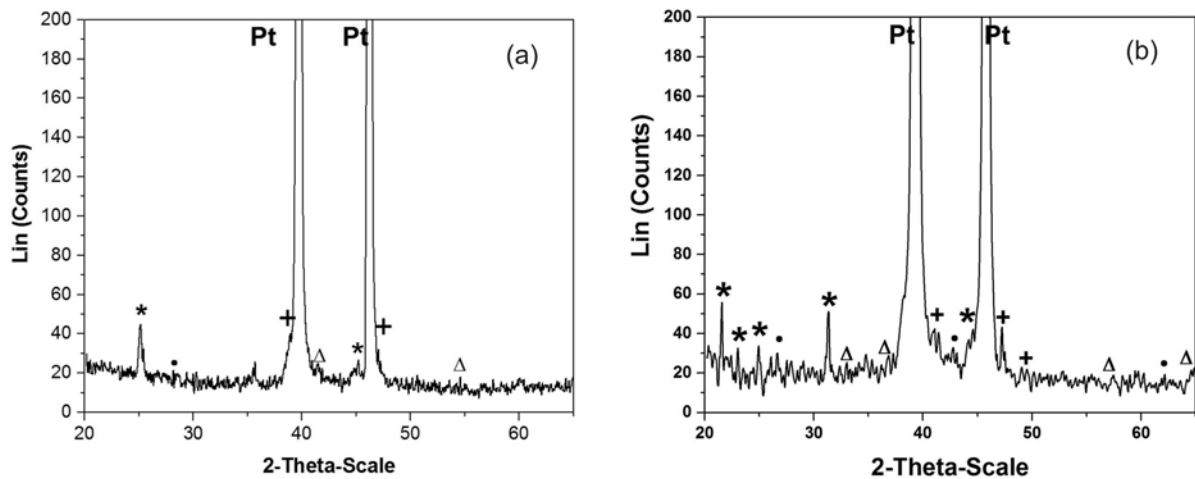

Fig. 6. Diffraction patterns of platinum sample after a) two and b) five hours of magnesium underpotential deposition at E_X = +80 mV vs. Mg in non-aqueous eutectic mixture $Mg(NO_3)_2 + NH_4NO_3$ at T = 450 K; a) and b) (+) (fct) – $MgPt_3$ [39]; (∗) (hcp) – Mg_3Pt [40]; (△) (bcc) – MgO_2 [41]; (●) – (fcc) MgO [42].

has not been completely determined for the Mg-Pt system.

The solubility of Pt in Mg appears to be negligible, and that of Mg in Pt has not been determined. However, the conductivity of a two-phase Mg-0.14 at.%-Pt alloy was measured, and it proved that the conductiv-

ity was less than that of pure Mg, so there was some solubility of Pt in Mg [44]. On the other side of the diagram the X-ray analysis of a two-phase Mg-Pt alloy (Mg-0.12 at.%-Pt), and the lattice parameters of Mg ($a = 0.32080$ nm and $c = 0.52103$ nm) and those of pure Mg ($a = 0.32088$ nm and $c = 0.52099$ nm) shows

T a b l e 2. The alloys identified on platinum samples after magnesium underpotential deposition at different times from non-aqueous eutectic mixture $Mg(NO_3)_2 + NH_4NO_3$ at $T = 450$ K

T (K)	Time (h)	Identified phase	System	Approximate composition (at.% Pt)
450	2	$MgPt_3$	hcp	≈ 71.6
450	5	$MgPt_3$	fct	≈ 71.6
	5	Mg_3Pt	hcp	≈ 25

to be very close to each other, indicating a very low solid solubility of Pt in Mg. An analysis of Mg-Pt binary system [44] suggests that the eutectic point is at 7.6 at.% Pt and 648 K (analogous to the Mg-Au system), and "at least" two intermediate phases: a homogeneous solid solution around the Mg_6Pt composition, and a stoichiometric Mg_3Pt compound (analogous to the Mg-Pd system).

Some authors [26] proposed that the experimental phases at compositions $MgPt_7$ and $Mg_{85}Pt_7$ were not evaluated because the structures have not been completely determined. At compositions Mg_2Pt and $MgPt_2$, phases may exist where none has been experimentally observed. While the $MgPt_2$ (Ga_2Hf structure) is found slightly above the tie line (~ 1.9 meV), the C16 structure is stable at Mg_2Pt. It is interesting to note, however, that an identical ordering of the phases in composition Mg_3Pt occurs in the chemically similar Mg-Pd system and that the stable ab initio and experimental phase at composition MgPd are L10.

Other authors [43] reported that magnesium platinum alloys were prepared by heating Mg and Pt in sealed Fe crucibles, then examined metallographically. From these examinations and a few thermal analyses, there were reports [44] of the existence of "at least" two intermediate phases: a homogeneous solid solution around the Mg_6Pt composition, and a stoichiometric Mg_3Pt compound (analogous to the Mg-Pd system). Different works [42] discovered two more intermediate phases, a MgPt compound and an ordered fct phase near 75 at.% Pt that coexists with Pt. On the Pt-rich side of the system, two cubic superlattice phases, $MgPt_3$ and $MgPt_7$ were found [45]. The alloys were prepared by reduction of MgO with H_2 in the presence of Pt between 1373 and 1673 K. $MgPt_3$ was prepared at 1373 K in the composition range 71.6 to 75.5 at.% Pt and $MgPt_7$ was formed in the temperature range 1473 to 1673 K in the composition range 85.5 to 89.7 at.% Pt [44]. It appears that the ordered fct phase near 75 at.% Pt reported by [39] and the ordered $MgPt_3$ phase of [45] are the same phases.

The alloys: hcp $MgPt_3$ and hcp Mg_3Pt, described in the above-cited literature, have been recorded in magnesium underpotential deposition experiments performed on platinum in used nitrate melts but at temperatures which are several hundred K lower (see Figs. 6a,b and Table 2). Which part of the magne-

sium adatoms formed by underpotential deposition on platinum surface participate in oxide formation and which diffuse into the substrate and contribute to alloy formation could not be concluded by linear sweep voltammetry, EDS or XRD results. LSV results indicated EDS and XRD results confirmed both magnesium-platinum alloy and magnesium oxide formation at the surface of the platinum electrode in nitrate melts used.

Equation (1) describes the process of magnesium oxide formation in the absence of water in the used melts [14, 15]. In addition, some novel results [31–33] suggest that every amount of reactive magnesium on the electrode surface in the presence of O^{2-} and OH^- anions very quickly turns into MgO. Therefore, the surface of the platinum working electrode becomes partially covered with MgO even in the first linear change of the potential from anodic end to cathodic end of the magnesium underpotential range. This, however, did not preclude a sufficient amount of magnesium underpotentially produced adatoms to participate in magnesium-platinum alloy formation by interdiffusion. Part of the magnesium ions in magnesium (II) oxide probably diffuse through the oxide layer to the platinum surface where they become discharged into magnesium adatoms which are then participating in the interdiffusion processes as well. Fast and unavoidable formation of insoluble MgO in the magnesium underpotential deposition range on platinum from used nitrate melts explains quasi-passivation of the working electrode and the lack of anodic current peaks on the voltammograms recorded.

4. Conclusions

The UPD of Mg on Pt substrate from magnesium nitrate melts used at potentials very close to 100 mV vs. Mg was established.

As a result of the magnesium underpotential deposition onto the platinum substrate from the nitrate melts used the formation of two alloys, Mg_3Pt and Pt_3Mg, was observed.

Alloys obtained were formed at the temperatures several hundred degrees Kelvin lower than the temperatures which are, according to the existing knowledge

on the binary Mg-Pt system, needed for their formation by thermal means.

It appears that underpotential deposition of the metals unsuitable for electrodeposition from aqueous electrolytes, like magnesium, can be performed even from nitrate melts at low temperatures and that it can lead to the formation of alloys in a controlled manner.

Acknowledgement

References

[1] Rokhlin, L.: In: Advances in Metallic Alloys. Volume 3. Eds.: Fridlyander, J. N., Eskin, D. G. New York, Taylor & Francis 2003.

[2] Friedman, P. A., Copple, W. B.: J. Mater. Eng. Perform.,*13*, 2004, p. 335. doi:10.1361/10599490419162

[3] Viestfrid, Y., Levi, M. D., Gofer, Y., Aurbach, D. J.: Electroanal. Chem., *576,* 2005, p. 183. doi:10.1016/j.jelechem.2004.09.034

[4] Eliezer, D., Aghion, E., Froes, F. H.: Advance Performance Materials, *5*, 1998, p. 201. doi:10.1023/A:1008682415141

[5] D'Errico, F., Kim, S. K., Garces, P. G., Giger, F.: JOM, *65*, 2013, p. 1293. doi:10.1007/s11837-013-0705-1

[6] Mezbahul-Islam, M., Mostafa, A. O., Medraj, M.: Journal of Materials, Article ID 704283, 2014. doi:10.1155/2014/704283

[7] Kierzek, A., Adamiec, J.: Archives of Metallurgy and Materials, *56*, 2011, p. 759. doi:10.2478/v10172-011-0084-y

[8] Kolb, D. M.: In: Advances in Electrochemical Science and Engineering. Eds.: Alkire, R. C., Kolb, D. M. Weinheim, Wiley-VCH 2001.

[9] Martinez, A. M., Haarberg, G. M., Borresen, B., Castrillejo, Y., Tunold, R.: J. Appl. Electrochem., *34*, 2004, p. 1271. doi:10.1007/s10800-004-1761-6

[10] Lu, Z., Schechter, A., Moshkovich, M., Aurbach, D.: J. Electroanal. Chem., *466*, 1999, p. 203. doi:10.1016/Soo22-0728(99)00146-1

[11] Wang, P., NuLi, Y., Yang, J., Feng, Z.: Surf & Coat Techn., *201*, 2006, p. 3783. doi:10.1016/j.surfcoat.2006.03.020

[12] Mamantov, G., Hussey, C. L., Marassi, R.: In: Techniques for Characterization of Electrodes and Electrochemical Processes. Eds.: Varma, R., Selamn, J. R. New York, John Wiley and Sons 1991.

[13] Bhatia, K., Sharma, R. C., Gaur, H. C.: Electrochim. Acta, *23*, 1978, p. 1367. doi:10.1016/0013-4686(78)80018-8

[14] Tkalenko, D. A.: Electrochemistry of Molten Nitrates. Kiev, Naukova Dumka 1983. (in Russian)

[15] Tkalenko, D. A.: Macrokinetics Cathode Processes Hydroxide and Nitrate Melts. Kiev, Naukova Dumka 1993. (in Russian)

[16] Ramana, K. V., Sharma, R. C., Gaur, H. C.: J. Chem. Engineer. Data, *31*, 1986, p. 288. doi:10.1021/je00045a009

[17] Ramana, K. V., Sharma, R. C., Gaur, H. C.: J. Chem. Engineer. Data, *35*, 1990, p. 293. doi:10.1021/je00061a020

[18] Ramana, K. V., Sharma, R. C., Gaur, H. C.: J. Chem. Engineer. Data, *35*, 1990, p. 418. doi:10.1021/je00062a013

[19] Vidu, R., Hirai, R., Hara, N.: Phys. Chem. Chem. Phys., *3*, 2001, p. 3320. doi:10.1039/b010250o .

[20] Radović, B. S., Edwards, R. A. H., Jovićević, J. N.: J. Electroanal. Chem., *428*, 1997, p. 113. doi:10.1016/S0022-0728(96)05050-4

[21] Radović, B. S., Cvetković, V. S., Edwards, R. A. H., Jovićević, J. N.: Kovove Mater., *48*, 2010, p. 159. doi:10.4149/km_2010_3_159

[22] Radović, B. S., Cvetković, V. S., Edwards, R. A. H., Jovićević, J. N.: Kovove Mater., *48*, 2010, p. 55. doi:10.4149/km_2010_1_55

[23] Stafford, G. L., Hussey, C. L.: In: Advances in Electrochemical Science and Engineering. Eds.: Alkire, R. C., Kolb, D. M. Weinheim, Wiley-VCH Verlag GmbH 2002.

[24] Cvetkovic, V. S., Bjelica, L. J., Vukicevic, N. M., Jovicevic, J. N.: CI&CEQ, *21*, 2015, p. 527. doi:10.2298/CICEQ141205009C

[25] Cvetković, V. S.: Underpotential Deposition of Magnesium from Nitrate Melts. Mitrovica, Zadužbina Andrejević – PMF K. 2012. (in Serbian)

[26] Taylor, R. H., Curtarolo, S., Hart, G. L. W.: Physical Review. B84 084101-1/084101-16, 2011. doi:10.1103/PhysRevB.84.084101

[27] Esbenshade, L. J., Barile, J. C., Fister, T. T., Bassett, L. K., Fenter, P., Nuzzo, G. R., Gewirth, A. A.: J. Phys. Chem. C, *119*, 2015, p. 23366. doi:10.1021/acs.jpcc.5b07825

[28] Vardar, G., Sleightholme, E. S. A., Naruse, J., Hiramatsu, H., Siegel, J. D., Monroe, W. C.: Appl. Mater. Interfaces, *6*, 2014, p. 18033. doi:10.1021/am5049064

[29] Chang, J., Haasch, T. R., Kim, J., Spila, T., Braun, V. P., Gewirth, A. A., Nuzzo, G. R.: ACS Appl. Mater. Interfaces, *7*, 2015, p. 2494. doi:10.1021/am507375t

[30] Biggs, T.: Metals Rev., *49*, 2005, p. 2. doi:10.1595/147106705X24409

[31] Amir, N., Chusid, O. V., Aurbach, D. G.: J. Power Sources, *174*, 2007, p. 1234. doi:10.1016/j.jpowsour.2007.06.206

[32] Martinez, A. M., Borresen, B., Haarberg, G. M., Catrillejo, Y., Tunold, R.: J. Electrochem. Soc., *151,* 2004, p. C508. doi:10.1149/1.1758814

[33] Brenner, A.: In: Advances in Electrochemistry and Electrochemical Engineering. Ed.: Tobias, C. W. New York, Interscience 1976.

[34] CRC Handbook of Chemistry and Physics. Boca Raton, CRC Press Inc. 2002.

[35] Kolb, D. M., Przasnyski, M., Gerischer, H.: J. Electroanal. Chem., *54*, 1974, p. 25. doi:10.1016/S0022-0728%2874%2980377-3

[36] Radović, B. S., Cvetković, V. S., Edwards, R. A. H., Jovićević, J. N.: Int J Mater Res., *102*, 2011, p. 59. doi:10.3139/146.110443

[37] Jovićević, N., Cvetković, V. S., Kamberović, Ž. J., Jovićević, J. N.: Metallurgical and Materials Transactions B, *44*, 2013, p. 106. doi:10.1007/s11663-012-9750-3

[38] Hume-Rothery, W., Smallman, R. E., Haworth, C. W.: The Structure of Metals and Alloys. 5th Edition. London, The Institute of Metals 1969.

[39] Stadelmaier, H. H., Hardy, W. K.: Z. Metallkd., *52*, 1961, p. 391.

[40] Range, K. J., Haffner, P.: J. Alloys Compd., *183,* 1991, p. 430. doi:10.1016/0925-8388(92)90764-Z

[41] Vannerberg, N. G.: Ark. Kemi, *14*, 1959, p. 99.

[42] Kondrashev, Y. D., Omeľchenko, Y. A.: Zh. Neorg. Khim., *9*, 1964, p. 512.

[43] Ferro, R., Rambaldi, G.: J. Less-Common Metals, *2*, 1960, p. 383. doi:10.1016/0022-5088(60)90047-3

[44] Nayeb-Hashemi, A. A., Clark, J. B.: Bulletin of Alloy Phase Diagrams, *6*, 1985, p. 533. doi:10.1007/BF02887151

[45] Bronger, W., Klemm, W.: Z. Anorg. Chem., *319*, 1962, p. 58. doi:10.1002/zaac.19623190110